AIMETA 2017
XXIII Conference
The Italian Association of Theoretical and Applied Mechanics
Luigi Ascione, Valentino Berardi, Luciano Feo, Fernando Fraternali and Antonio Michele Tralli (eds.)
Salerno, Italy, 4–7 September 2017

A 6DOF/HIL SETUP FOR WIND TUNNEL HYBRID TESTS ON A 1/75 SCALE MODEL OF A 10 MW FLOATING WIND TURBINE

Ilmas Bayati[1], Marco Belloli[1], Alan Facchinetti[1] and Hermes Giberti[2]

[1]Politecnico di Milano, Department of Mechanical Engineering
Via La Masa 1, 20156, Milano
{ilmasandrea.bayati,marco.belloli, alan.facchinetti}@polimi.it

[2] Universita degli Studi di Pavia, Department of Industrial and Information Engineering
Pavia, Italy
hermes.giberti@unipv.it

Keywords: FOWT, HIL, Wind Tunnel, Robotcs, Wind Energy

Abstract. *This paper deals with the design of a 6 degrees-of-freedom (DoF) robot for Hardware-In-The-Loop wind tunnel tests of floating offshore wind turbines (FOWT) and its experimental implementation. This setup allow to perform wind tunnel tests with a physical scale model of a wind turbine and to provide the motion at the base of the tower thanks to a 6-DoF Hexaslide robot with parallel kinematics. The motion is given consistently with real time combination of measurements (aerodynamic forces) and computations (hydrodynamic forces). The paper presents an overview of the design process of the robot as well as a description of the corresponding integrated numerical model based on MSC-Adams/Adwimo/MATLAB-Simulink co-simulation environment to account for the complete dynamic system (robot, wind turbine, control, HIL algorithm). The structural model of the wind turbine has been verified against the experimental modal analysis on the scale model. The complete model has been validated against a reduced order experimental setup (2-DoF), in terms of the aerodynamic forces computed in dynamic conditions (imposed motion tests) as well as HIL methodology effectively implemented for various conditions (free decay in still water and air, irregular sea state with wind). The main results of such a validation are reported showing promising extension outputs considering the ongoing extension to 6-DoF, making this tool valuable of numerical benchmark and wind tunnel design of experiments (DoE).*

1 INTRODUCTION

The work is part of the wider project, LIFES50+ [1], funded by the EU under the H2020 programme, which aims at providing cost effective technology for floating substructures for 10 MW wind turbines, at water depths greater than 50 m, also through innovative real time Hardware-In-The-Loop (HIL) experimental approach (computations/measurements) with combined wind tunnel (Politecnico di Milano, [2], [3]) and ocean basin (Sintef Ocean, [4], [5]) model tests. The motivation lies on the desire to move from combined wind-wave model tests [6] on FOWTs to wind- or wave-only experiments, respectively in wind tunnel and ocean basin, through hybrid/HIL approach. This is helpful in exploiting separately the advantages of the respective tests and to overcome the inevitable scaling issues [6], testing systems subjected to the combined effect of gravity dependent loads (waves) and aerodynamic loads (wind turbine), which cause the impossibility to keep respectively the Froude and Reynolds similitude between full and model scale, i.e. Froude-Reynolds conflict, see [7]. The HIL system for wind tunnel application [8] herein presented, takes advantage of the physical wind turbine scale model developed for LIFES50+ project, [9] and [10], which is an 1/75 aero-servo-elastic scale model of the DTU 10 MW reference wind turbine [11]. This turbine is installed on a 6-DoF mechanical robot, which moves the base of the tower based on the integration of a dynamic model accounting for the hydrodynamic forces of the simulated floating system and the aerodynamic forces of the wind tunnel model, measured by a dynamometric balance between the robot and the wind turbine scale model.

This paper presents an overview of the design of the 6-DoF HIL setup, which is being finalized at the time of this paper, the HIL methodology adopted, the integrated corresponding numerical model (design of experiments) and its experimental validation with a reduced-order (2DoF) setup.

2 6-DoF robot design

The design of the 6-DoF parallel kinematic machine, called Hexaslide, to perform HIL experiments [12], was carried out considering various aspects, which are reported in the following. First of all, the attachment point between mobile platform and scale model, referred to as TCP (*tool-center-point*) was required to be kept as low as possible for leaving the greatest room to the wind turbine scale model (this 6-DoF/HIL setup is placed in the Atmospheric Boundary Layer test section of Politecnico di Milano wind tunnel [8], which is 13,84 m wide x 3,84 m high). This allows to build bigger wind turbine scale models for having the lowest discrepancy of Reynolds number as possible, with respect to the full scale prototype, up to a limit linked to the aerodynamic blockage effect typically considered in wind tunnel experiments. Moreover, the zone near the ceiling of the test section, is characterized by a boundary layer in which the nominal wind speed reduces, so it was important that wind turbine blade tips were staying outside this region, approximately of 30 cm. The reference wind turbine [11] was scaled using

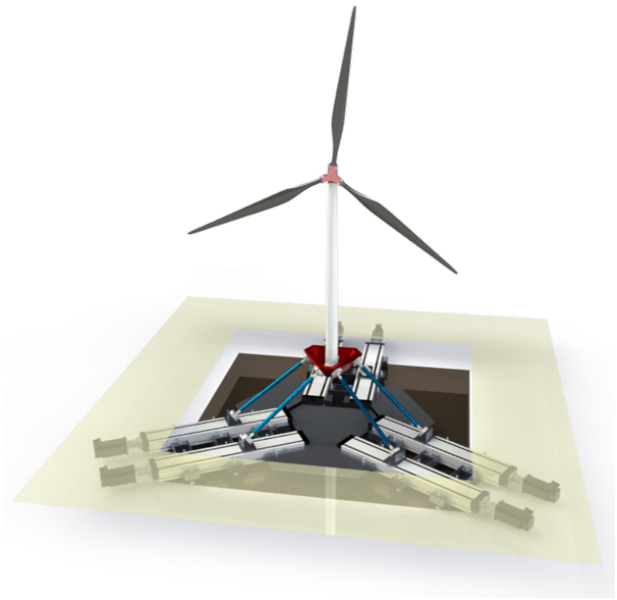

Figure 1: Hexaslide, Politecnico di Milano 6-DoF robot for wind tunnel tests on floating wind turbines with HIL approach

a scale factor of 75, considered a good compromise among these issues.

In the preliminary phase of the design, the hypothesis of adopting a serial robot was considered, since these manipulators are definitely the most diffused in the market and do not bring any problem in terms of workspace dimensions. However, in serial manipulator the errors of each joint is summed up consequently increasing the inaccuracy of the positioning of the end-effector (TCP). These considerations, in addition to the need of having a low TCP, led to consider parallel kinematic manipulators (PKM) as the most valid alternative. Nevertheless, the performance of these machines strictly depends on their dimensions, therefore a straightforward comparison among different families was quite hard, [14]. The size of their working volume is lower than that of serial robots, but these machines are characterized by a high stiffness thanks to the peculiar distribution among the links of the loads acting on the end-effector. Furthermore, some PKM as the Hexaslide are characterized by having spherical or cardanic joints at the ends of their links, so the loads to which the links are subjected to are exclusively axial. Also, in PKM, the combination among the errors/backlash of each joint, leading to the inaccuracy of the end-effector, is way more complex with respect to serial robots, resulting in a lower sensitivity of the positioning errors of the end-effector. Among PMK, the Hexaslide was chosen for this project.

The Hexaslide robot is made of a mobile platform connected to six linear guides by means of six links of fixed length, so that six independent kinematic chains can be identified belonging to the PUS family. A detailed description of 6-DoF PUS PKMs can

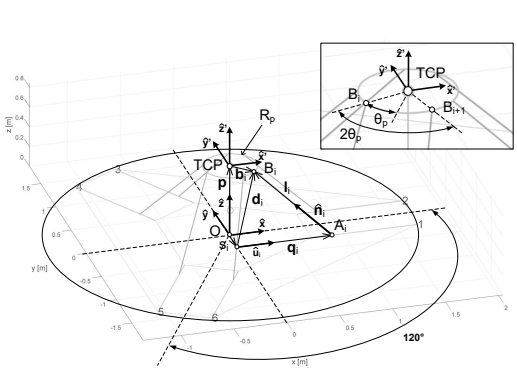

(a) 6-DoF Hexaslide kinematic scheme

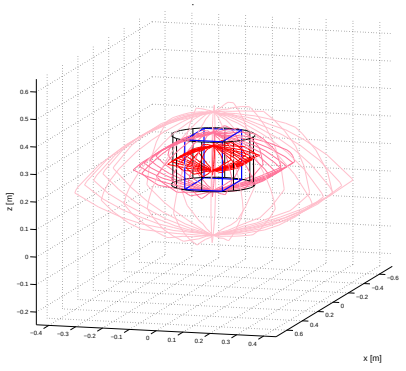

(b) Various work TCP workspaces (red) during the optimization process, compared to the target (blue)

Figure 2: Hexaslide design

be found in [16, 17]. The six linear guides are organized into three couples of parallel transmission units, each one out of phase by $120°$ with respect to the vertical z axis.

With reference to Figure 2a, given the TCP position and the mobile platform orientation, $\Theta = \{\alpha, \beta, \gamma\}$, it is possible to find each slider position, q_i, by performing the inverse kinematics analysis, for the i-th kinematic chain it is possible to write:

$$\mathbf{l}_i = \mathbf{d}_i + q_i \hat{\mathbf{u}}_i \qquad \text{with} \qquad \mathbf{d}_i = \mathbf{p} + [R]\mathbf{b}'_i - \mathbf{s}_i \tag{1}$$

The [R] matrix is the rotational matrix used to switch from the mobile frame to the fixed one, and it is function of the platform orientation Θ. After a few passages it can be written:

$$q_i = \mathbf{d}_i^T \hat{\mathbf{u}}_i \pm \sqrt{\mathbf{d}_i^T (\hat{\mathbf{u}}_i \hat{\mathbf{u}}_i^T - [I])\mathbf{d}_i + l_i^2} \tag{2}$$

Once solved the inverse kinematics it is possible to find the relationship between the slider velocity and the velocity of the TCP. It can be shown that for the i-th kinematic chain the following expression holds:

$$\hat{\mathbf{n}}_i^T \hat{\mathbf{u}}_i \dot{q}_i - [\hat{\mathbf{n}}_i^T \quad (\mathbf{b}_i \times \hat{\mathbf{n}}_i)^T]\mathbf{W} = 0 \tag{3}$$

where $\mathbf{W} = [\dot{x},\, \dot{y},\, \dot{z},\, \omega_x,\, \omega_y,\, \omega_z]^T$ is a vector containing both the translational and angular components of TCP velocity. Considering all the six links the previous relationship can be expressed through the Jacobian matrix $[J]$ as:

$$\mathbf{W} = [J]\dot{\mathbf{q}} \tag{4}$$

The Jacobian matrix *J* represents the relationship between the sliders velocity and the TCP velocity. Under the hypothesis of small displacements it is possible to use the

Jacobian matrix to relate the small variations of the sliders position to the variation of the robot pose as follows:

$$\Delta \mathbf{X} = [J]\Delta \mathbf{q} \tag{5}$$

This relationship allows to compute the TCP positioning due to the linear units displacements. In order to define the geometry of the final Hexaslide an optimization was performed, as thoroughly explained in [13], to get the optimal parameters among the length of the links l_i, the semi-distance between the sliders s_i, the end-effector's platform radius R_p and the semi-angle between two consecutive links of each pair, with respect to the TCP, θ_p, and the vertical position p of the workspace center (nominal TCP). The optimization was based on multi-objective genetic algorithm minimizing the workspace volume within the target one (Fig. 2b: $\Delta x = 300mm$, $\Delta y = 150mm$, $\Delta z = 150mm$, $\Delta\alpha = 10°$, $\Delta\beta = 16°$, $\Delta\gamma = 6°$) , which the robot is not able to cover. This optimization process accounts for geometrical constraints (interference between links), kinematic constraints (each point of the effective workspace is effectively reachable) and kinetostatic constraints (limitation of the actuation force at the sliders due to each TCP's pose), [18]. In Fig. 2b a qualitative view of the effective workspaces reached by different Hexaslide configurations during the optimization process, is reported.

The optimal sizing of the motor-reducer units actuating the sliders (ball-screw drive actuators), relied on the dynamic analysis of the optimal Hexaslide, based on Monte Carlo simulations, considering contemporary sinusoidal motions along the 6 degrees of freedom, of various frequencies, amplitudes and relative phase shifts, [19]. The dynamic model adopted for this analysis, was a MSC/Adams model accounting for the flexibility of the components used during the structural design process to assess also the dynamic response of the robot itself [20], designed for being as stiff as possible. This model was integrated in the complete numerical setup (robot/wind turbine/HIL) explained in the following.

3 Reduced-order experimental 2 DoF benchmark setup

Being the Hardware-In-The-Loop procedure for testing floating wind turbines in wind tunnel a non-trivial task, in terms of hydrodynamic modelling, robot's control and real-time numerical-experimental consistency, a numerical model 6-DoF model of the setup was developed either for design support tool and for a reliable design-of-experiment tool for wind tunnel tests. Nevertheless, in order to validate such a model, a reduced-order (2-DoF) setup was taken into account to perform some preliminary measurements, Fig. 3. This system also allowed to tune a proper HIL methodology on a simpler system, which could have been eventually extended to 6-DoF Hexaslide. Such 2-DoF system is based on two hydraulic actuators that move the base of the wind turbine's base along surge and pitch directions, thanks to a slider-crank mechanism; a dynamometric load balance is placed between the mechanism end effector and the wind turbine scale model.

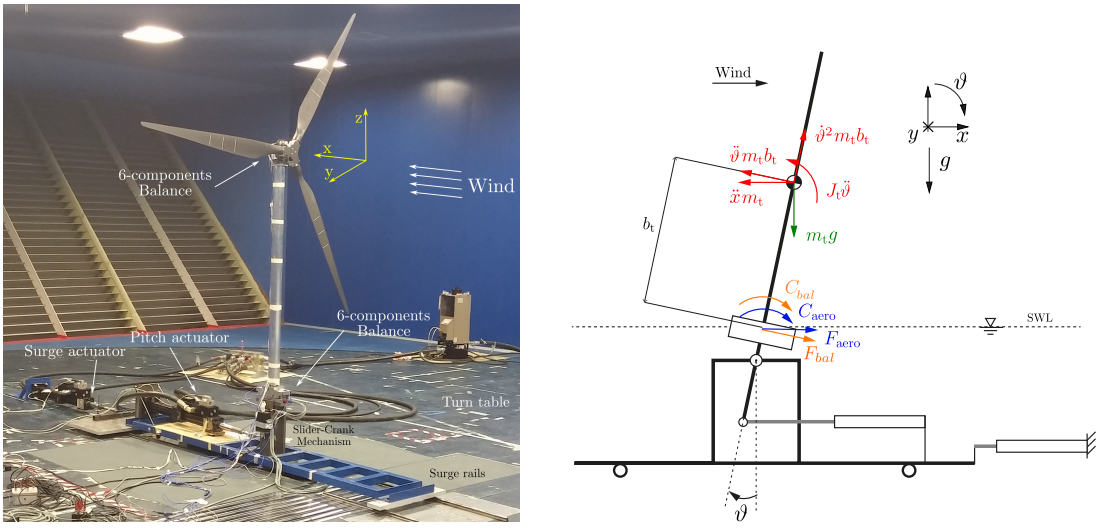

(a) 2-DoF/HIL system

(b) 2-DoF/HIL system conventions

Figure 3: 2-DoF/HIL system based on hydraulic actuators, for surge and pitch motions

As mentioned the HIL experimental approach relies on hybrid setup in which the overall forces acting on the simulated floating system are partially hydrodynamic ones ($\underline{F}_{hydro}$, computed) and partially aerodynamic ones ($\underline{F}_{aero}$measured). Therefore, the overall system dynamics can be described by the 2-DoF set of equations:

$$\big[[M_s] + [A_\infty]\big]\underline{\ddot{x}} + [R_s]\underline{\dot{x}} + [K_s]\underline{x} = \underline{F}_{hydro} + \underline{F}_{aero} \tag{6}$$

where M_s is the floating system mass matrix, A_∞ the infinite-frequency hydrodynamic added mass matrix, R_s is the linear addedd damping matrix (from ocean basin tests) and K_s is the floating system stiffness matrix (composed of hydrostatic restoring and gravitational stiffness). $\underline{F}_{hydro}$ is computed and it is composed of radiation forces, diffraction forces and the ones due to the mooring line system. More details about the various contributions of $\underline{F}_{hydro}$ can be found in [21]. Nevertheless, $\underline{F}_{aero}$ are derived by the measurement of the load balance placed in between the motion mechanism and the tower's base, $\underline{F}_{bal}$, however it contains also other contributions. With reference to Fig. 3b, for a generic (positive) state of the motion surge and pitch variables x and ϑ, the forces measured by the balance $\underline{F}_{bal}$ are due to inertia, gravitational stiffness and aerodynamic forces (and moments) as it can be written in Eq. 7:

$$\underline{F}_{bal} = -\begin{bmatrix} m_t & b_t m_t \\ b_t m_t & b_t^2 m_t + J_t \end{bmatrix}\underline{\ddot{x}} + \begin{bmatrix} 0 & m_t g \\ 0 & m_t b_t g \end{bmatrix}\underline{x} + \underline{F}_{aero} \tag{7}$$

where mass, moment of inertia and CoG position of the wind turbine t (m_t, J_t and b_t) have been experimentally derived by means of surge- and pitch-only imposed tests at

different frequencies and amplitudes, to decrease as much as possible their uncertainty. Furthermore, for the sake of simplicity and without loss of significant information, the surge force measured by the balance F_{bal}, is assumed to be along x even if it is in the balance's reference system (rotating), considering small ϑ angles at issue (linearization, e.g. $cos(\vartheta) \approx 1$). The same for the inertial force due to surge $\ddot{x}m_t$ which is considered along the measurement direction of the balance.

Nevertheless, if these values (m_t, J_t and b_t) were all and perfectly matching the model scaling requirements, which is hardly achievable, the model could be modified with respect to the formulation in Eq. 6, as follows

$$\begin{aligned}\big[[M_{pl}] + [A_\infty]\big]\underline{\ddot{x}} + [R_s]\underline{\dot{x}} + [K_{pl}]\underline{x} &= \underline{F}_{hydro} + \underline{F}_{aero} \\ &= \underline{F}_{hydro} + \underline{F}_{bal} + \underline{F}_c \end{aligned} \tag{8}$$

where *pl* stands for "platform" meaning that on the left hand-side of Eq. 8 only the platform terms are considered, whereas the wind turbine inertial and gravitational terms are already considered (measured) on the right hand-side by the vector $\underline{F}_{bal}$, with the only exception of a single-term correction vector $\underline{F}_c$:

$$\underline{F}_c = \begin{bmatrix} 0 & -m_t g \\ 0 & 0 \end{bmatrix} \underline{x} \tag{9}$$

Beyond this small exception (Eq. 9), Eq. 8 would tell that the balance would measure exactly the forces exchanged between the wind turbine and the platform, included the aerodynamic forces. However, this is hardly reachable, then, instead of Eq. 8, Eq. 6 still has to keep the whole system matrices and becomes:

$$\begin{aligned}\big[[M_s] + [A_\infty]\big]\underline{\ddot{x}} + [R_s]\underline{\dot{x}} + [K_s]\underline{x} &= \underline{F}_{hydro} + \underline{F}_{aero} \\ &= \underline{F}_{hydro} + \underline{F}_{bal} + \underline{F}_c^{'} \end{aligned} \tag{10}$$

with a correction element $\underline{F}_c^{'}$ which cancels all the inertial and gravitational terms out of Eq. 7 to get aerodynamic forces only from balance measurements (getting rid of the inertial and gravitational terms more related to the wind turbine physical scale model than the simulated wind turbine). Furthermore, there is also a methodological reason why Eq. 8 cannot be adopted, also if the physical model were ideally matching the target perfectly: this is the case of a non-Froude scaling approach in the tests. In fact, keeping the Froude similitude, as in the ocean basin tests, the acceleration scale factor turns out to be equal to 1 (affecting g and $\underline{\ddot{x}}$), so the measurements (Eq. 7) would be all consistent with the whole simulation Eq. 8; whereas if Froude does not hold, the acceleration factor is different from 1, so the correction to the measurements must be performed either way, as in Eq. 10.

Nevertheless, the correction $\underline{F}_c^{'}$ to the inertial and gravitational terms of the measurements $\underline{F}_{bal}$ (Eq. 7), requires the exact knowledge of the effective system's state (i.e.

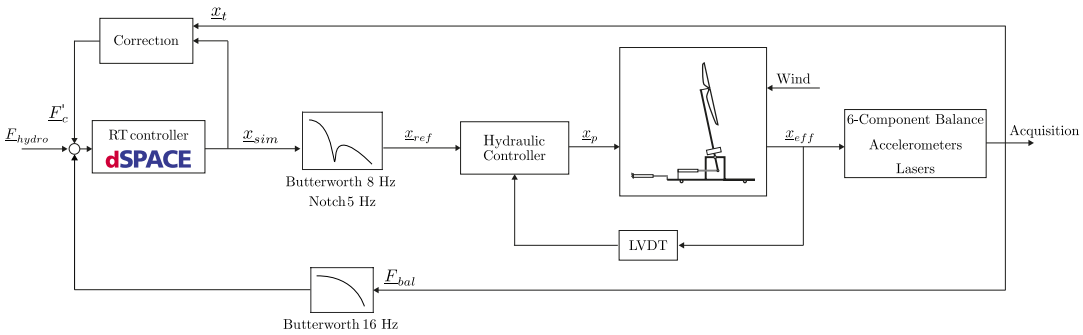

Figure 4: General control scheme of the 2-DoF HIL setup

$\ddot{\underline{x}}_t$ and $\underline{x}_t$) at every time step and introduces the need of managing further measured signals (accelerations and position feedback), which turned out to be troublesome [22], also considering the increasing complexity when this setup is being extended to 6 DoF, [3]. Therefore, the effective wind turbine state $\underline{x} = \underline{x}_t$, was assumed to be equal to the simulated one $\underline{x} = \underline{x}_{sim}$ of the RT numerical model (Fig. 4), so that:

$$\begin{aligned} \underline{F}_{aero} =& \underline{F}_{bal} + \underline{F}_c' = \\ =& \underline{F}_{bal} + \begin{bmatrix} m_t & b_t m_t \\ b_t m_t & b_t^2 m_t + J_t \end{bmatrix} \ddot{\underline{x}}_{sim} + \begin{bmatrix} 0 & -m_t g \\ 0 & -m_t b_t g \end{bmatrix} \underline{x}_{sim} \end{aligned} \tag{11}$$

Further information about how these issues were addressed, can be found in [21] and [22], as well as a more detailed description of the measurement chain, which is herein merely recalled Fig.4. The same considerations are being carried out for the 6-DoF robot being finalized, which will be relying on the same load balance and measurement/HIL approach.

4 Numerical model and experimental validation

In Fig.5 a general overview of the numerical model developed in the environment MSC Adams-Adwimo is reported. More specifically, the FEM/MultiBody software MSCAdams has been used for the modelling the robot, also during the reported design phases, and the wind turbine plug-in Adwimo was also coupled, with the possibility to have a numerical model of the wind turbine very close to the real scale model prototype. Moreover, in order to have the most reliable numerical model representing the wind tunnel experiment, a Matlab/Simulink co-simulation environment was developed to allow the inclusion in the simulation of the wind turbine controller (main shaft and blade's pitch) effectively deployed on the real-time (RT) hardware and, most importantly, the same HIL algorithm downloaded onto the dSpace RT controller. The latter performs the integration of the equation of motion (Eq.6), including the aerodynamic force handling (Eq.11) providing the position of the TCP (6-DoF, 6 signals) to the robot controller, which translates them into 6 commands to the sliders due the the inverse kinematics, as

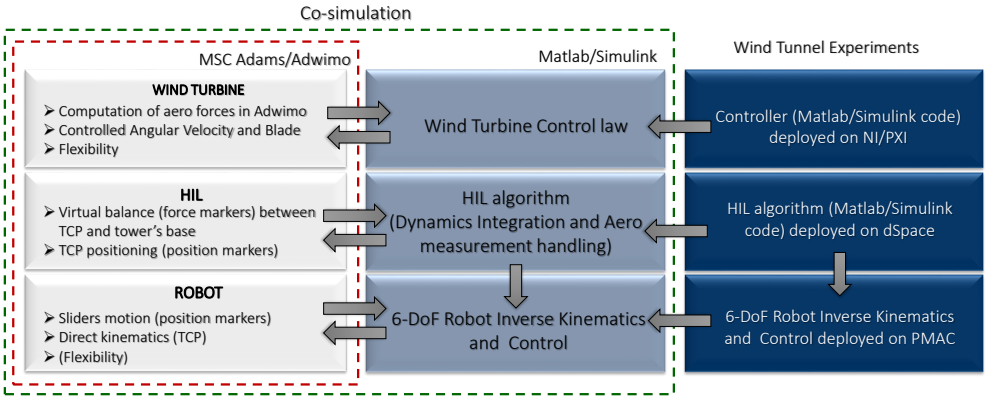

Figure 5: Adams/Adwimo numerical model scheme

actually done by the hardware.

The experimental validation of such numerical model was performed by considering the following items:

- Wind turbine's structure: verification against experimental modal analysis
- Aerodynamics of wind turbine: steady and unsteady (imposed motion)
- HIL methodology: irregular sea state and constant wind

As reported more extensively in [7] and [10], after the realization of the wind turbine scale model a modal analysis was conducted to verify that the correctness of the natural frequencies of the aero-elastic scale model had been effectively reached, showing good agreement with the expectations. At this point the flexibility was introduced in the MSC Adams/Adwimo. As an example, in Fig.6 the first collective collective blade flap-wise mode of $15.47Hz$ against the obtained experimental value of $15.58Hz$, [7], which makes the numerical model reliable in an aero-elastic sense.

Good agreement was found with regard to the steady aerodynamics (e.g. prediction of the steady rotor thrust due to constant wind, Fig.7a). Furthermore, imposed motion tests, at different amplitudes and frequencies, were performed to investigate unsteady aerodynamics phenomena of floating wind turbines in dynamic conditions. Previous works, [23] and [24], has shown discrepancies between the experiments and the numerical counterpart, adopting NREL/AeroDyn to model the wind turbine scale model. These discrepancies are still being investigated, nevertheless, since Adwimo plug-in implements AeroDyn as well, numerical imposed motion tests, with the reported model,

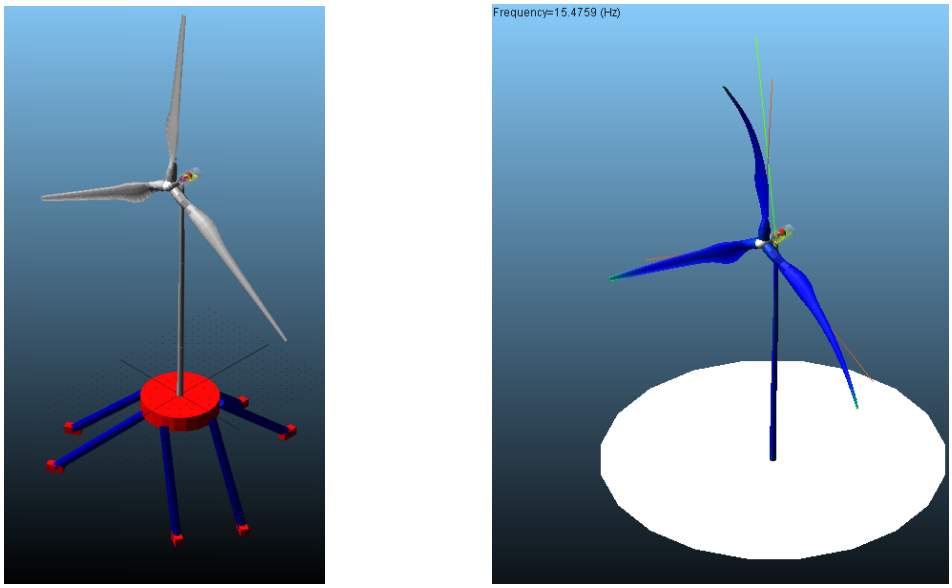

Figure 6: Numerical model of the 6-DoF/HIL setup in MSC Adams/Adwimo environment (left), fist collective blade flap-wise mode (right)

Wind Speed (m/s)	**Experiment (N)**	**NREL/AeroDyn (N)**	**Adams/Adwimo (N)**
2.33	1.79	0.84	0.62
3.67	3.44	0.81	0.55
5.30	3.29	1.84	1.92

Table 1: Amplitudes of variation about the steady thrust force values, for imposed surge motion tests (sine waves)

were performed. A sample of significant cases are reported in Tab.1, for below, rated and above rated wind speeds showing the same trend of lower numerical variation around the steady thrust force value, compared to the experiments.

After having checked, by means of free decay tests in still water, that the mass distribution of the numerical model was effectively giving the same rigid-motion natural frequency of the platform (see, Fig.7b), irregular sea states were simulated as during the wind tunnel experiments, as reported in [21], considering the OC5 semi-submersible floating wind turbine, considering the 6-DoF MSC Adams/Adwimo model, although considering only surge and pitch motion, as in the experiments Fig.3a. In Fig.8 the assessment in irregular sea is reported, with reference to Power Spectral Densities (PSD) of the the pitch degree-of-freedom. The random-phase sea spectra adopted during wind tunnel HIL experiments were the same provided to the simulations (see Fig.8). The graphs are reported in the model-based frequency domain and show a good overall

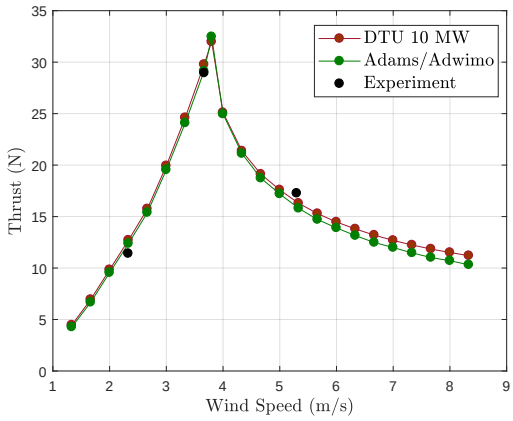

(a) Rotor thrust force

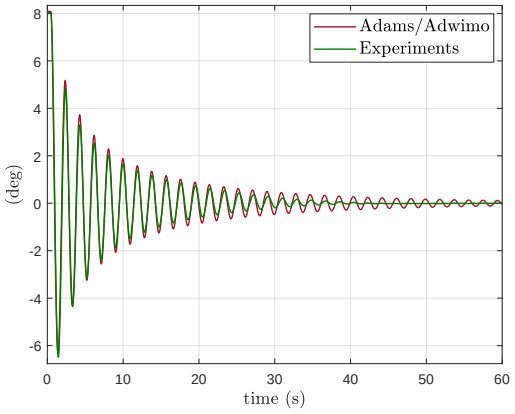

(b) Platform pitch free decay

Figure 7: Wind Turbine performance (left) and still water free decay of the floating system(right)

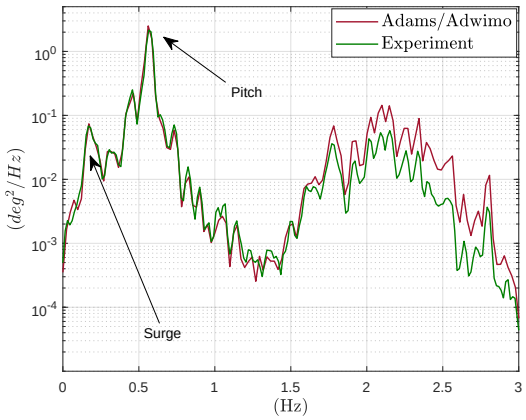

(a) PSD of pitch motion in irregular sea with no wind

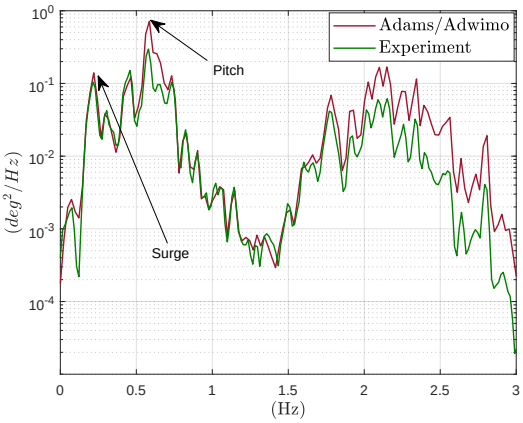

(b) PSD of pitch motion in irregular sea with wind

Figure 8: Numerical-Experimental comparison for irregular sea state.

agreement. More specifically, it can be observed that in the wave-frequency range, approximately between $1.5 - 3Hz$ the discrepancies between the model and the experiments are not depending on the presence of wind. As it has been documented in [21] and [22] this is likely due to the readiness (frequency bandwidth) of the hydraulic actuation system, which will possibly improved in the 6-DoF electro-mechanical based actuation system of the Hexaslide. Furthermore, the low frequency range, where the rigid-motion platform natural frequencies of a semi-submersible floating system are designed to be, are forced by the second-order wave diffraction forces. In case of no wind (8a) the surge and pitch natural frequency peaks are perfectly overlapped, showing the perfect numerical reproduction of the methodology, whereas in case of wind blowing constantly on the rotor 8b, the experiments, seems to be more damped. The quantitative and systematic analysis of such differences between the model and the experiments is still object of investigation by the authors.

5 Conclusions and ongoing developments

The paper presented an overview of the design process of the robot, the corresponding integrated numerical model based on Adams/Adwimo/Simulink co-simulation environment to account for the complete dynamic system (robot, wind turbine, control, HIL algorithm). The model has been validated against a reduced order experimental setup (2-DoF), with regard to the aerodynamic forces computed in the numeric environment as well as the HIL methodology effectively implemented for various conditions (free decay in still water and air, irregular sea state with wind). The main results of such a validation are reported showing promising extension for the extension to 6-DoF and making this tool valuable of numerical benchmark and design of experiments (DoE) in that it allows to assess directly the control strategies of the wind turbine, of the robot and of the HIL algorithm, which are effectively deployed onto the real-time hardware (Matlab/Simulink code).

At this point the validated numerical tool is being used for assessing the correctness of the overall methodology on the 6-DoF system as well as specific load cases in the late stages of the robot constructions, to drive decisions at component level (i.e. custom-made joints dimensioning). Moreover, in order to make the developed tool even more reliable, a particular attention will be made to reproduce the closest simulations accounting also for the effective data exchange rates among the various moduli (Fig.5, e.g. sampling frequencies) reflecting the effective hardware performance.

6 Aknowledgments

This project has partially received funding from the European Union's Horizon 2020 research and innovation programme under grant agreement no 640741.

REFERENCES

[1] ”H2020 LIFES50+ Project”, http://lifes50plus.eu/

[2] Bayati, I., Belloli, M., Facchinetti, A., Giappino, S., ”Wind tunnel tests on floating offshore wind turbines: A proposal for hardware-in-the-loop approach to validate numerical codes” (2013) Wind Engineering, 37 (6), pp. 557-568, DOI: 10.1260/0309-524X.37.6.557.

[3] I. Bayati, M. Belloli, D. Ferrari, F. Fossati, H. Giberti, ”Design of a 6-DoF robotic platform for wind tunnel tests of floating wind turbines”, Energy Procedia, 2014, DOI: 10.1016/j.egypro.2014.07.240.

[4] Sauder, T. and Chabaud, V. and Thys, M. and Bachynski, E.E. and Sæther, L.O., ”Real-time hybrid model testing of a braceless semi-submersible wind turbine. Part I: The hybrid approach”, Proceedings of the International Conference on Offshore Mechanics and Arctic Engineering - OMAE, 2016, DOI: 10.1115/OMAE2016-54435.

[5] Bachynski, E.E. and Thys, M. and Sauder, T. and Chabaud, V. and Sæther, L.O., ”Real-time hybrid model testing of a braceless semi-submersible wind turbine. Part II: Experimental results”, Proceedings of the International Conference on Offshore Mechanics and Arctic Engineering - OMAE, 2016, DOI: 10.1115/OMAE2016-54437.

[6] Robertson, A.N. and Jonkman, J.M. and Goupee, A.J. and Coulling, A.J. and Prowell, I. and Browning, J. and Masciola, M.D. and Molta, P., ”Summary of conclusions and recommendations drawn from the deepcwind scaled floating offshore wind system test campaign”, Proceedings of the International Conference on Offshore Mechanics and Arctic Engineering - OMAE, 2013, DOI:10.1115/OMAE2013-10817

[7] Bayati, I. and Belloli, M. and Bernini, L. and Giberti, H. and Zasso, A., ”On the scale model technology for floating offshore wind turbines”, IET Renewable Power Generation, 2017, DOI: 10.1049/iet-rpg.2016.0956

[8] Politecnico di Milano Wind Tunnel (GVPM), http://www.windtunnel.polimi.it/.

[9] I. Bayati, M. Belloli, L. Bernini, E. Fiore, H. Giberti, A. Zasso, On the functional design of the DTU10 MW wind turbine scale model of LIFES50+ project, Journal of Physics Conference Series 753(5), October 2016. DOI: 10.1088/1742-6596/753/5/052018

[10] I. Bayati, L. Bernini, M. Belloli, A. Zasso, Aerodynamic design methodology for wind tunnel tests of wind turbine rotors, Journal of Wind Engineering and Industrial Aerodynamics, June 2017, 10.1016/j.jweia.2017.05.004

[11] C. Bak et Al, The DTU 10-MW Reference Wind Turbine,Technical University of Denmark, DTU Wind Energy, Denmark, 2013.

[12] Bayati I., Belloli M., Ferrari D., Fossati F., Giberti H., "Design of a 6-DoF Robotic Platform for Wind Tunnel Tests of Floating Wind Turbines", *Energy Procedia Journal*, vol. 53, pp. 313-323, 2014.

[13] Fiore, E., Giberti, H., "Optimization and comparison between two 6-DoF parallel kinematic machines for HIL simulations in wind tunnel" (2016) MATEC Web of Conferences, 45, art. no. 04012, DOI: 10.1051/matecconf/20164504012

[14] Merlet, J.P., 2006, "Parallel Robots", 2 ed., Springer.

[15] Fiore, E., Giberti, H., Ferrari, D., "Dynamics Modeling and Accuracy Evaluation of a 6-DoF Hexaslide Robot", (2015) Proceedings of the 33rd IMAC, pp. 473-479.

[16] Bonev, Ilian Alexandrov, 1998, "Analysis and Design of a 6-DOF 6-PRRS Parallel Manipulators", M.Sc. thesis, GIST, South Korea.

[17] Bonev, Ilian Alexandrov, 2001, "A geometrical method for computing the constant-orientation workspace of 6-PRRS parallel manipulators", Mechanism and Machine Theory, 36, pp. 1-13.

[18] Legnani, G., Tosi, D., Fassi, I., Giberti, H., Cinquemani, S., "The Point of Isotropy and other Properties of Serial and Parallel Manipulators", *Mechanism and Machine Theory*, vol. 45, no. 10, pp. 1407-1423, 2010.

[19] Fiore, E., Giberti, H., Bonomi, G. "An innovative method for sizing actuating systems of manipulators with generic tasks" (2017) Mechanisms and Machine Science, 47, pp. 297-305. DOI: 10.1007/978-3-319-48375-7-32.

[20] Fiore E., Giberti H. (2017) A Montecarlo Approach to Test the Modes of Vibration of a 6-DoF Parallel Kinematic Simulator. In: Harvie J., Baqersad J. (eds) Shock and Vibration, Aircraft/Aerospace, Energy Harvesting, Acoustics and Optics, Volume 9. Conference Proceedings of the Society for Experimental Mechanics Series. Springer, DOI: 10.1007/978-3-319-54735-0-33

[21] I. Bayati, M. Belloli, A. Facchinetti, Wind tunnel 2-DoF hybrid/HIL tests on the OC5 Floating Offshore Wind Turbine, 36th International Conference on Ocean, Offshore and Arctic Engineering, Trondheim (Norway), 2017, OMAE2017-61763

[22] Ambrosini, S., Bayati, I., Belloli, M., Facchinetti, A., "Methodological and technical aspects of a 2DoF/HIL setup for wind tunnel tunnel tests of floating systems", "Journal of Dynamic Systems, Measurement, and Control", forthcoming, 2017.

[23] I. Bayati, M. Belloli, L. Bernini, A. Zasso, Wind tunnel validation of AeroDyn within LIFES50+ project: imposed Surge and Pitch tests, Journal of Physics Conference Series 753(9), October 2016. DOI: 10.1088/1742-6596/753/9/092001

[24] I. Bayati, M. Belloli, L. Bernini, A. Zasso, A formulation for the unsteady aerodynamics of floating wind turbines, with focus on the global system dynamics, 36th International Conference on Ocean, Offshore and Arctic Engineering, Trondheim (Norway), 2017, OMAE2017-61925